Radon concentration in room air

Fortgeschrittenen-Praktium, Physik Department, TUM

Anil Berkay Adigüzel
Matr. 03745052

Berke Mert
Matr. 03738893

Tianrui Xu
Matr. 03716809

November 2022

Contents

1 Introduction

Radon is a radioactive gas that forms naturally when the radioactive metals uranium, thorium, or radium decay in rocks, soils, and groundwater. It is one of the largest natural sources of radiation to which a typical human is exposed[1]. The main purpose of the experiment is to determine the radon concentration in the air. Radon can cling onto the dust particle, this means we can make measurements using the dust particles. For this, we used an air filter to collect the dust from the room, and measure the activity of the dust using a high purity germanium detector.

2 Theory

Substances containing unstable nuclei lose energy via radiation to reach a more stable state, this process is called radioactive decay. The radioactive decay is determined as follows,

$$\frac{dN}{dt} = -\lambda N \tag{1}$$

where N is the number of particles and λ is defined one divided by the lifetime, τ.
In some cases, radioactive substances go through a series of radioactive decays to reach a stable state. The decay chain refers to these sequential decays. In a decay chain, the number of a certain isotope is given by the difference between radioactive decay of mother nuclei and the isotope in question. The number of atoms of the i-th isotope is therefore given by

$$\frac{dN_i}{dt} = \lambda_{i-1}N_{i-1} - \lambda_i N_i. \tag{2}$$

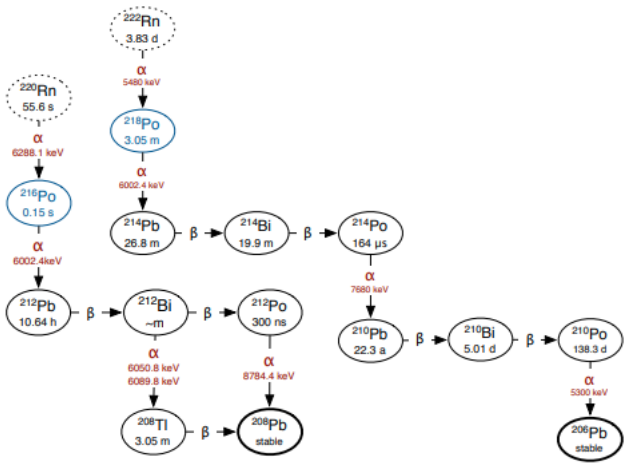

Figure 1: The decay chains of ^{232}Th and ^{238}U starting from their radon daughter. Taken from [1]

The Figure 1 shows a part of the decay chains of ^{232}Th ^{238}U. S. Since the lifetime of the primordial Th and U is much longer than those of all the daughters, the decay chains are in secular equilibrium;that for arbitrary isotopes i and j in the same chain

$$\lambda_i N_i = \lambda_j N_j \tag{3}$$

holds true as long as the chain is not broken [1].
The primordial isotopes ^{232}Th and ^{238}U go through radioactive decay to form radon, a radioactive noble gas. Radon is released from the earth's crust into the air. The decay products of radon have the capability of clinging onto dust particles. The amount of radioactive material in the air, therefore, can be determined by the filtering of the air.
The collected number of atoms of the direct daughter Polonium, Po, in a volume of filtered air, V, is given by the following equation:

$$\frac{dN_{Po}}{dt} = \epsilon_f \rho_{Po} V - \lambda_{Po} N_{Po} \tag{4}$$

where ϵ_f is the filtration efficiency and ρ_{Po} is the Po atoms per cubic meter.
The next daughter in the decay chain is lead, Pb. The number of Pb atoms in the filter is determined by the accumulation from the air, decay of its mother nuclei, Po, and the decay of Pb itself, which leads to the following relation:

$$\frac{dN_{Pb}}{dt} = \lambda_{Po} N_{Po} + \epsilon_f \rho_{Pb} V - \lambda_{Pb} N_{Pb} \tag{5}$$

The decay of a radon daughter isotope is determined in this experiment via the measurement of gamma radiation. The number of detected lead decays can be used to calculate the Pb concentration in the air by using the following equation [1]:

$$\begin{aligned} N_\gamma = {} & \epsilon_f \epsilon_d R \rho_{Pb} V \\ & \cdot \Big[\{ \frac{1}{\lambda_{Po}} + \frac{1}{\lambda_{Pb}} + \frac{\lambda_{Pb}}{\lambda_{Po}(\lambda_{Po} - \lambda_{Pb})} + \frac{\lambda_{Po} e^{-\lambda_{Pb} T_f}}{\lambda_{Pb}(\lambda_{Pb} - \lambda_{Po})} \} \, (e^{-\lambda_{Pb} t_1} - e^{-\lambda_{Pb} t_2}) \\ & + \{ \frac{\lambda_{Pb}}{\lambda_{Po}(\lambda_{Pb} - \lambda_{Po})} (1 - e^{-\lambda_{Po} T_f}) \} e^{(-\lambda_{Po} t_1} - e^{-\lambda_{Po} t_2} \Big] \end{aligned} \tag{6}$$

where the variables are labeled as follows:

V	: The air throughput of the filter unit in m^3/s
ϵ_d	: The detection probability for a gamma particle at this energy
R	: The branching ratio for emission of a gamma particle of this energy
T_f	: The duration for which the air was filtered.
t_1, t_2	: The start and stop time of the data collection in seconds from the time the air filter was turned off

3 Experimental Setup & Procedure

Before starting with the data collection, we need to exclude the background radiation from our raw data coming from radon daughter isotopes in close vicinity of the detector. For this, the background spectrum is measured a day before the real experiment.
We trap dust particles with an air filter unit in a HEPA filter and operate it for about one hour to be efficient with our time, since the number of impulses per unit time decreases significantly at this time mark, compare Figure 9. After the filter process, we note down T_f and V.
During the filter process, we connect the High Purity Germanium Detector(HPGe) to the data detection software MC^{2}Analyzer. The experimental setup and the setup of the HPGe is shown in Figures 2 and 3.
Germanium detectors are semiconductors with a p-i-n structure, in which the depleted region (i) is sensitive to ionized radiation (such as gamma rays). When these gamma rays interact within the depleted region, electron-hole pairs are produced, which are swept by the p and n electrodes. This charge is converted into a voltage pulse by a charge-sensitive preamplifier, which then gets sent into one of 60000 channels in the DTS780 and digitized in the software MC^{2}Analyzer. We can increase the number of produced charge-carriers

by applying a high reverse bias voltage on the Germanium.
Germanium has low band gap, thus we have to cool it to reduce thermal generation of the charge-carriers and therefor reduce noise of the reverse leakage-current. This increases the resolution of the HPGe, so we can have clearly distinct decay lines of the radon daughters.
The germanium detector registers counts per given energy. Yet, in order to see the explicit dependency between channel number and energy, we need to calibrate the energy with a source with known decay lines. It needs to be in range of 50 keV to 300 keV, which is why we choose ^{133}Ba, and we choose ^{60}Co so we can find a good fit to our calibration curve.

After the filter process, we take out the HEPA filter, fold it as small as possible and start the data collection process, after which we note down t_1 and t_2.

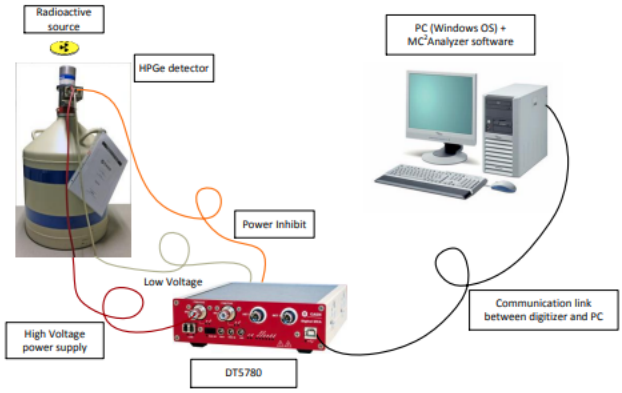

Figure 2: Experimental Setup

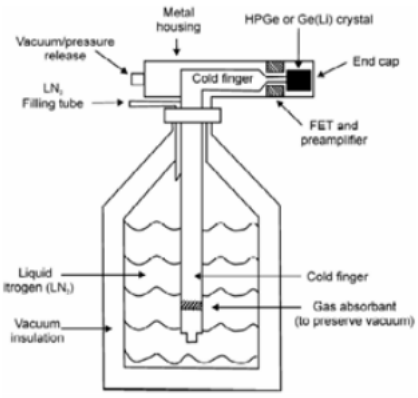

Figure 3: HPGe Detector

4 Analysis & Results

4.1 Energy calibration of the detector

Before calibration, we normalize all the collected data to counts per second, and subtract the data for cobalt and barium with the background noise. For calibration, we first plot the counts against the channels, and use $scipy.findpeak$ to roughly locate the peaks. Then, we use a Gaussian distribution function regardless of the offset to determine the exact location of the peak.

$$G(x) = A \exp\left(\frac{(x-\mu)^2}{2\sigma^2}\right), \tag{7}$$

The fit parameters are listed in table 1, in which μ represents the location of each peak. Notice that in order to let $scipy.curve\_fit$ work, we scale down the x individually with an extra factor. According to counts, we can correlate the peaks with specific decay lines and their theoretical energy level in table (1). By using linear regression, as shown in figure 4, we obtain the calibration curve

$$y = 0.310\,13(1)\,\text{keV} \cdot x - 68.064\,39(2914)\,\text{keV}. \tag{8}$$

The residue of the fit curve from each data point can be found in figure 5. The difference is in 10^{-5} order, thus we consider the fit being very precise. Regarding the systematic uncertainty in calibration, despite using the Gaussian distribution function, the position of each peak may have offset compared to theoretical value. This won't change the slope of the linear regression, however, is still relevant in the constant part. We can reduce it by increasing the time of detection.

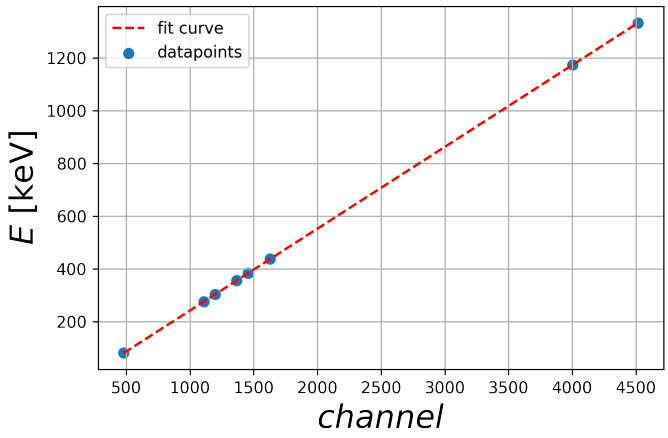

Figure 4: calibration curve

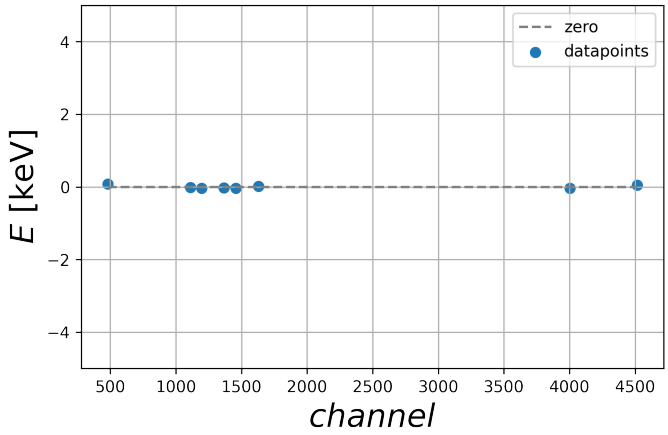

Figure 5: residue of calibration curve

4.2 Efficiency of the detector

The detector only can measure a certain amount of the solid angle because of its structure. Therefore, it is wise to determine the detection efficiency. For this purpose we calculated the expected number of counts, $N_\gamma^{expected}$, for the peaks in calibration curve, refer to table 2.
To calibrate the detection efficiency, we calculate the ratio of the measured gamma decays, $N_\gamma^{measured}$, to the expected value,

$$\epsilon_d = \frac{N_\gamma^{measured}}{N_\gamma^{expected}}. \tag{9}$$

We can determine $N_\gamma^{measured}$ by fitting Gaussian distributions over the decay lines, and integrating over the channel numbers in the range $\mu \pm 2\sigma$. After, we plotted the efficiency against the energy as shown in Figure 6.

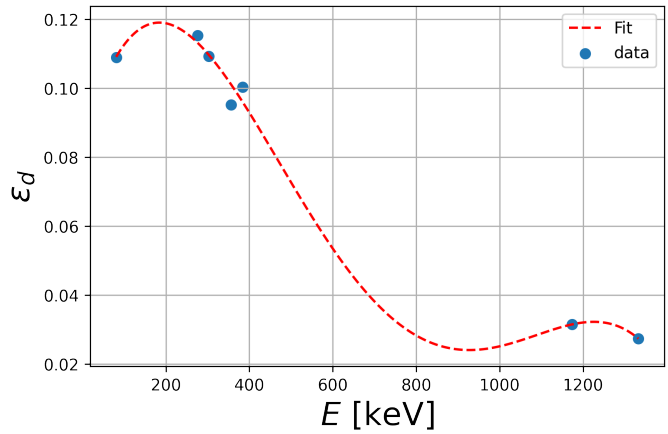

Figure 6: Curve fit of the detection efficiency plotted against energy

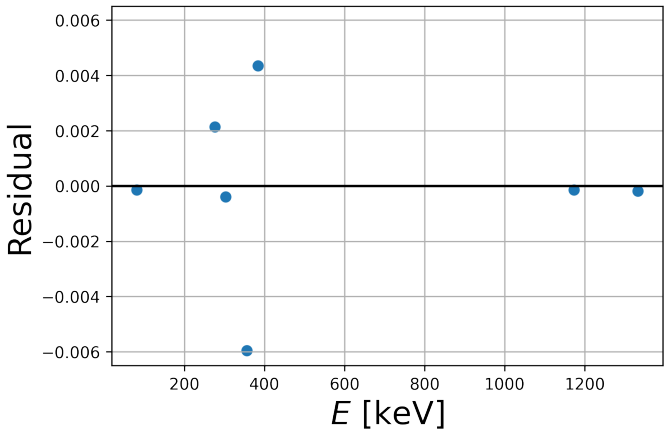

Figure 7: Residue of the curve fit

Note, that t Using a polynomial fit we determined the efficiency as a function of energy:

$$\epsilon_d(E) = -5.182 \cdot 10^{-13} \cdot E^4 + 1.615 \cdot 10^{-9} \cdot E^3 - 1.589 \cdot 10^{-6} \cdot E^2 + 4.338 \cdot 10^{-4} \cdot E + 8.358 \cdot 10^{-4} \quad (10)$$

4.3 Radon concentration in room air

Before going on with our calculations, we first need to process our raw data of the filter paper spectrum. For this, we scale down the y-axis of both the filter paper spectrum and the background spectrum to counts per second, and then subtract the background from the filter paper spectrum. Additionally, we have to convert our x-axis from channel number to energy with our energy calibration curve from before. This gives us a final plot in figure (8).

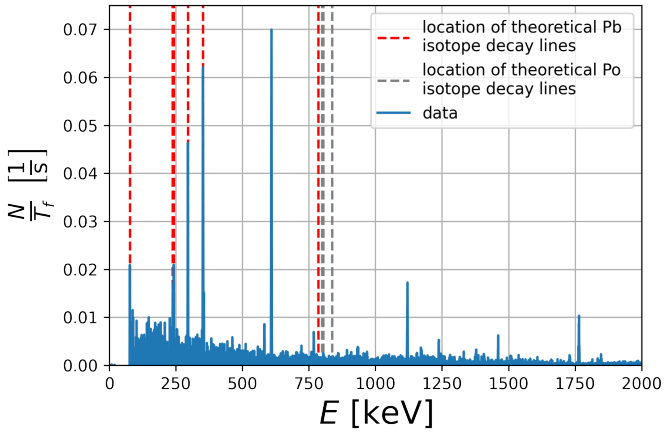

Figure 8: Filter paper spectrum with location of theoretical Polonium and Lead isotopes decay lines

There are no significant Polonium decay lines in our spectrum. This can be explained by the negligibly small half-life and branching ratios of the polonium isotopes. We also want to point out that we have to

exclude the 77.1 keV γ-line, since we don't know how much both ^{214}Pb and ^{212}Pb contribute to the number of counts per second.
We can determine the net count rate, N_γ, of the relevant lead peaks by subtracting the background from the filter paper spectrum and then dividing the peaks with the bin width of the histogram. We can then rearrange 6 for ρ_{Pb} to calculate the concentration of Lead in room air, see table 3.
To get the lead concentration in room air we make a weighted average of ρ_{Pb}, this gives us

$$\rho_{Pb-212} = 1170.23 \pm 3.10 \ \frac{\text{atoms}}{\text{m}^3} \tag{11}$$

$$\rho_{Pb-214} = 806.61 \pm 64.42 \ \frac{\text{atoms}}{\text{m}^3}. \tag{12}$$

Assuming secular equilibrium, we can at last calculate the radon concentrations in room air according to equation (3)

$$c_{Rn-220} = (21.17 \pm 0.56) \ \frac{\text{mBq}}{\text{m}^3} \tag{13}$$

$$c_{Rn-222} = (0.35 \pm 0.03) \ \frac{\text{Bq}}{\text{m}^3}. \tag{14}$$

The results are well within the theoretical range of 0 to 20 $\frac{\text{Bq}}{\text{m}^3}$ in Munich and therefore satisfactory [3].

5 Literature

References

[1] Physics department TUM,
Radon concentration in room air
URL: https://www.ph.tum.de/academics/org/labs/fopra/docs/userguide-02.en.pdf

[2] Table of Isotopes, The Lund/LBNL Nuclear Data Search, Version 2.0, February 1999, SY.F. Chu. L.P. Ekström and R.B. Firestone

[3] Bundesamt fuer Strahlenschutz,
Radon in Innenräumen in Deutschland
URL: https://www.bfs.de/DE/themen/ion/umwelt/radon/karten/innenraeume.html#:~:text=Die%20H%C3%B6he%20der%20Radon%2DKonzentrationen,m%C3%B6glich%2C%20kommen%20jedoch%20selten%20vor.

6 Appendix

6.1 Figures

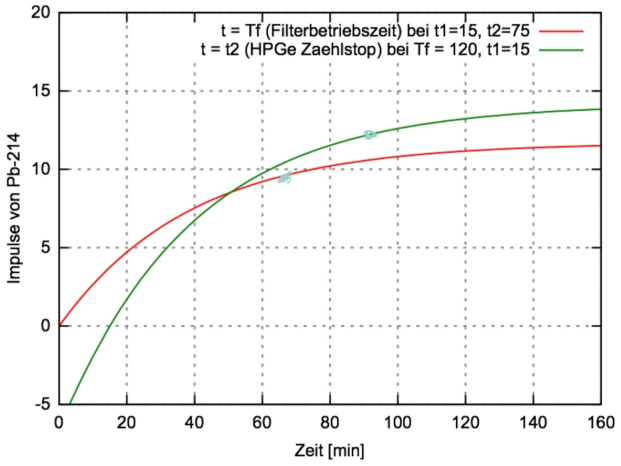

Figure 9: Impulses of ^{222}Ra N_γ

Isotope	Half-life	Decay Gamma-ray Energy (keV)	Branching Ratio (%)	Decay Mode
^{220}Rn	55.6 s	549.7	0.095	α 100%
^{216}Po	0.15 s	804.9	0.0018	α 100%
^{212}Pb	10.64 hr	77.1	17.5	β⁻ 100%
		238.6	43.6	
		300.1	3.34	
^{212}Bi	60.55 min	727.2	6.65	β⁻ 64.1%
		785.4	1.11	
		1620.6	1.51	
^{212}Bi	60.55 min	39.9	1.10	α 35.9%
^{212}Po	2.98×10^{-7} s			α 100%
^{208}Tl	3.05 min	72.8	2.03	β⁻ 100%
		75.0	3.43	
		84.8	1.18	
		277.4	6.80	
		510.8	21.6	
		583.1	86.0	
		763.1	1.64	
		860.4	12.0	
		2614.6	99.8	
^{208}Pb	stable			

Figure 10: Properties of ^{220}Rn daughters

Isotope	Half-life	Decay Gamma-ray Energy (keV)	Branching Ratio (%)	Decay Mode
^{222}Rn	3.82 d			α 100%
^{218}Po	3.11 min	837.0	0.0011	α 99.98% β$^-$ 0.02%
^{214}Pb	26.8 min	77.1	10.8	β$^-$ 100%
		241.9	7.46	
		295.2	19.2	
		351.9	37.1	
		785.9	1.09	
^{214}Bi	19.9 min	609.3	46.1	β$^-$ 99.98%
		665.5	1.56	α 0.02%
		768.4	4.88	
		806.2	1.23	
		934.1	3.16	
		1120.3	15.0	
		1155.2	1.69	
		1238.1	5.92	
		1281.0	1.47	
		1377.7	4.02	
		1401.5	1.39	
		1408.0	2.48	
		1509.2	2.19	
		1661.3	1.15	
		1729.6	3.05	
		1764.5	15.9	
		1847.4	2.12	
		2118.5	1.21	
		2204.1	4.99	
		2447.7	1.55	
^{214}Po	1.64x10^{-4} s	799.7	0.0104	α 100%
^{210}Tl	1.3 min	298	80	β$^-$ 100%
		797.7	100	
		860	7	
		1070	12	
		1110	7	
		1210	17	
		1316	21	
		2010	7	
		2360	8	
		2430	9	

Figure 11: Properties of ^{222}Rn daughters

6.2 Tables

Table 1: Table showing the fit parameter for isotopes ^{133}Ba, and ^{60}Co

Isotope	Energy [keV]	A	μ	σ [10^{-5}]	Factor of x
^{133}Ba	80.9971(14)	5.890(109)	0.48039(6)	264.67(6)	1000
	276.398(2)	1.172(26)	1.11073(7)	274.79(7)	1000
	302.853(1)	3.028(29)	1.19612(3)	258.09(3)	1000
	356.017(2)	8.742(43)	1.36748(2)	263.54(2)	1000
	383 851(3)	1.440(9)	1.45730(2)	268.97(2)	1000
	437.014(8)	0.525(6)	4.07131(9)	672.87(9)	400
^{60}Co	1173.237(4)	7.628(37)	1.000650(5)	85.725(4)	4000
	1332.501(5)	6.487(52)	1.128968(8)	87.772(8)	4000

Table 2: Table showing the branching ratio, expected counts and the corresponding energy for isotopes ^{133}Ba, and ^{60}Co

Isotope	Energy [keV]	Branching ratio	Expected Counts
^{133}Ba	53.161(1)	0.02199(23)	20.51(23)
	79.6139(26)	0.0262(6)	24.44(57)
	80 9971(14)	0.3406(27)	318(3)
	276.398(2)	0.07164(22)	66.84(37)
	302.853(1)	0.1833(6)	171.02(98)
	356.017(2)	0.6205(19)	579(3)
	383 851(3)	0.0989(3)	92.31(52)
^{60}Co	1173.237(4)	0.999736(7)	1990.50(19)
	1332.501(5)	0.999856(4)	1990.73(19)

Table 3: Net count rate, N_γ, and concentration ρ_{Pb} for the relevant Lead isotopes

Isotope	μ [keV]	μ_{Theo} [keV]	N_γ	ρ_{Pb}[Bq/m^3]
^{214}Pb	242.207(10)	241.9	1905.75	904.39 ± 2.38
	295.350(3)	295.2	4392.51	852.61 ± 2.34
	351.997(1)	351.2	6374.21	696.12 ± 2.07
^{212}Pb	238.571(17)	238.6	2672.56	1170.23 ± 3.10